HYDROLOGICAL PROCESSES
*Hydrol. Process.* (2011)

(wileyonlinelibrary.com) DOI: 10.1002/hyp.8046

# Integrated cave drip monitoring for epikarst recharge estimation in a dry Mediterranean area, Sif Cave, Israel

Nathan A. Sheffer,[1,2]* Moty Cohen,[3] Efrat Morin,[4] Tamir Grodek,[4] Alex Gimburg,[5] Einat Magal,[6] Haim Gvirtzman,[1] Manuela Nied,[7] Daniel Isele[7] and Amos Frumkin[4]

[1] *The Institute of Earth Sciences, The Hebrew University of Jerusalem, Jerusalem, Israel*
[2] *Bureau of Economic Geology, The University of Texas at Austin, Texas*
[3] *Robert H. Smith Faculty of Agriculture, Food and Environment, The Hebrew University of Jerusalem, Rehovot, Israel*
[4] *The Department of Geography, The Hebrew University of Jerusalem, Jerusalem, Israel*
[5] *Regional R&D Center, Science Park, Ariel, Israel*
[6] *Geological Survey of Israel, 30 Malkhe Israel st., Jerusalem, 95501, Israel*
[7] *Institute of Hydrology, University of Freiburg, Fahnenbergplatz 79098 Freiburg, Germany*

## Abstract:

Understanding recharge mechanisms and controls in karst regions is extremely important for managing water resources because of the dynamic nature of the system. The objective of this study was to evaluate water percolation through epikarst by monitoring water flow into a cave and conducting artificial irrigation and tracer experiments, at Sif Cave in Wadi Sussi, Israel from 2005 through 2007.

The research is based on continuous high-resolution direct measurements of both rainfall and water percolation in the cave chamber collected by three large PVC sheets which integrate drips from three different areas (17, 46, and 52 $m^2$). Barrels equipped with pressure transducers record drip rate and volume for each of the three areas. The combined measured rainfall and cave data enables estimation of recharge into the epikarst and to better understand the relationship of rainfall-recharge. Three distinct types of flow regimes were identified: (1) 'Quick flow' through preferential flow paths (large fractures and conduits); (2) 'Intermediate flow' through a secondary crack system; and (3) 'Slow flow' through the matrix. A threshold of ~100 mm of rain at the beginning of the rainy season is required to increase soil water content allowing later rainfall events to percolate deeper through the soil and to initiate dripping in the cave. During winter, as the soil water content rises, the lag time between a rain event and cave drip response decreases. Annual recharge (140–160 mm in different areas in the cave) measured represents 30–35% of annual rainfall (460 mm). Copyright © 2011 John Wiley & Sons, Ltd.

KEY WORDS cave drips; percolation; recharge; vadose karst; artificial tracers; epikarst

*Received 13 February 2010; Accepted 28 January 2011*

## INTRODUCTION

Karst aquifers are conceptualized as having three forms of effective porosity; primary porosity of the matrix, secondary porosity of the fractures and fissures, and tertiary porosity where dissolution enlarged flow paths allow for rapid and turbulent flow (Worthington and Ford, 1999). In telegenetic carbonate aquifers, the primary porosity is reduced, and rendered ineffective at transmitting water. Water percolating through the vadose zone of telegenetic karst travels along two primary pathways: rapid conduit flow—'Quick flow', through the karst systems and large fractures (Ford and Williams, 2007; Frumkin, 1984) and capillary flow—'Slow flow', through fissures (Eaton and Bixler, 1987). Quinlan *et al.* (1996) describe karst systems as having a triple porosity of conduit flow, fissure flow, and matrix flow. In many cases it is difficult to distinguish fissure flow from matrix flow, therefore the two types of Quick flow and Slow flow are most commonly used.

Recharge estimation is important for understanding the water cycle, contaminant transport, and for water management. However, monitoring water in the vadose zone and estimating groundwater recharge is one of the most complicated tasks in the hydrological cycle (Hogan *et al.*, 2004; NRC, 2004). Continuous water content measurement using Time Domain Reflectometry (TDR) (e.g. Dahan *et al.*, 2007; Rimon *et al.*, 2007) or neutron activation (e.g. Koons and Helmke, 1978; Sophocleous, 1991) enable point study on the rate of water transmission through the vadose zone. Recharge was estimated at local and regional scales using DReAM (Daily Recharge Assessment Model; a water budget model) for perched springs in the Israeli Western Mountain Aquifer (WMA) and the entire WMA, respectively (Sheffer, 2009; Sheffer *et al.*, 2010). Automated monitoring from either a single or a group of speleothems studies were conducted at several sites such as Stump Cross Caverns, Yorkshire (Baker and Brunsdon, 2003) and Edwards Plateau, Texas (Gregory *et al.*, 2009). Tracers such as fluorescent dyes and environmental isotopes in the vadose zone at many sites showed an order of magnitude range in recharge rates over 7–70 m/yr which was attributed to different flow

---

*Correspondence to: Nathan A. Sheffer, The Institute of Earth Sciences, The Hebrew University of Jerusalem, Jerusalem, Israel.
E-mail: nathan@geologist.com

systems Quick flow and Slow flow, arid *versus* humid climate forcing, and variations in storage in the soil and epikarst, e.g. Mendip Hills, England (Friederich and Smart, 1982), Israel (Even *et al.*, 1986), Niaux, France (Bakalowicz and Jusserand, 1987), Pennine karst, England (Bottrell and Atkinson, 1992), Slovenia (Kogovšek, 1997), and Mt Carmel, Israel (Arbel Y, *et al.*, 2008).

The innovation in this study is the direct integrated cave dripping measurements. The study of the water percolating through epikarst at Sif cave in Israel, integrates hundreds of points over an area of approximately 120 m$^2$ of the cave ceiling. This is unlike previously mentioned work and many others which concentrated on collecting drips from either a single speleothem or a defined group of speleothems.

The objective of this study is to estimate recharge at Sif cave. This will be carried out by measuring water infiltration through the vadose zone, using mass balance of rain and cave drip, defining contributing areas to the sites and by conducting irrigation experiments with tracer test.

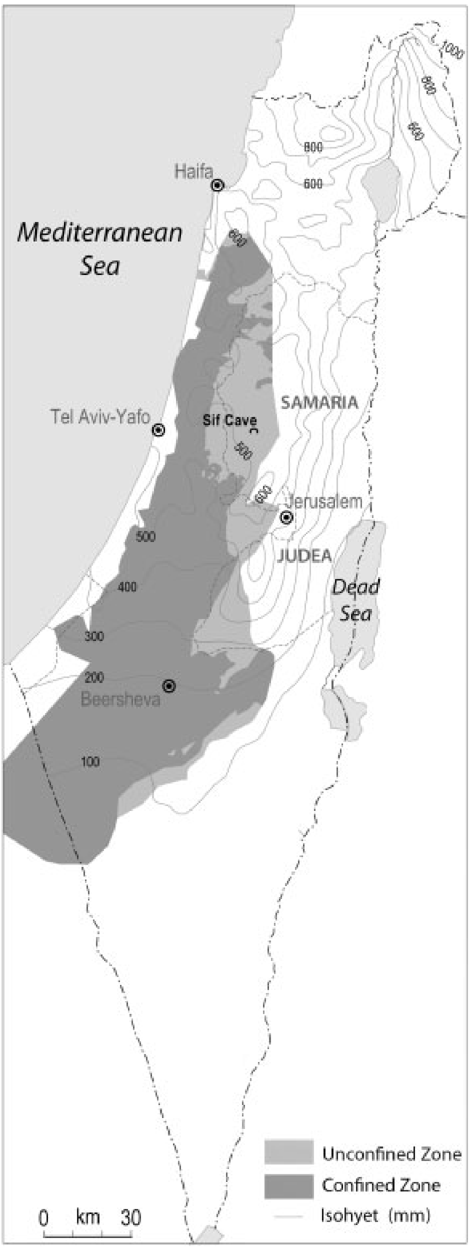

Figure 1. Location map of Sif cave. The shaded area represents the Israeli Western Mountain Aquifer (WMA) with the light shaded unconfined zone representing the recharge zone. Sif Cave is located within the recharge zone of the WMA

## STUDY SITE

### *Vicinity*

Sif cave is located in Central Israel, near the town of Ariel (Figure 1). The cave was formed in telogenetic mature dolomitic limestone of Weradim Formation, Cenomanian (late Cretaceous) age, in the upper part of the carbonate Judea Group (Arkin, 1967). The bedrock went through deep burial, associated with diagenesis that included compaction, leading to negligible matrix permeability followed by uplift and erosion of overlying beds. Mild tectonic deformation, associated with regional uplift, is reflected in two faults close to the cave (a few hundred meters away), but not within it. Fractures are tight, 0·5–5 m apart. The bedding is massive, dipping a few degrees to WNW. Typical to the region, this chamber cave formed under the water table by hypogene and phreatic water (Fischhendler and Frumkin, 2008; Frumkin and Fischhendler, 2005). Most of the cave ceiling is covered by speleothems, so speleogenetic morphology is hardly observed, although some dissolutional features visible on the ceiling indicate that it has survived from the original speleogenesis.

Sif Cave is located within the recharge area of the WMA. This aquifer provides approximately 20% of the fresh water supply of Israel (Gvirtzman, 2002). The regional water table in the vicinity of the cave is ~100 m below the land surface. The soil is patchy terra rossa (Committee on Soil Classification Israel, 1979), up to tens of cm deep. Vegetation is sparse, due to thousands of years of anthropogenic impact (mainly agriculture and deforestaion), which increased recently due to modern development, and the relatively dry climate.

The Mediterranean climate of the study area is characterized by hot, dry summers (June–August) and cool, rainy winters, extending from October to early May, with rainfall peaks in December through February (~70% of the rain). Mean annual rainfall at the study site is 550 mm/yr (Goldreich, 1998). The annual evapotranspiration (ET) averages around 65–75% of annual rainfall (Goldreich, 1998; Gvirtzman, 2002). Drainage basins with normally dry river beds of fluviokarst type concentrate subaerial runoff only during rare high-intensity rainfall events. These floods are monitored downstream, but the autogenic infiltration fraction of the rainfall has not been measured.

### *Sif cave*

Sif cave is an isolated karst chamber type cave (*sensu* Frumkin and Fischhendler, 2005), 27 m in diameter (570 m$^2$). The ceiling thickness is 3–11 m (Figure 2), and the chamber ceiling height varies from 2 to 7 m. The

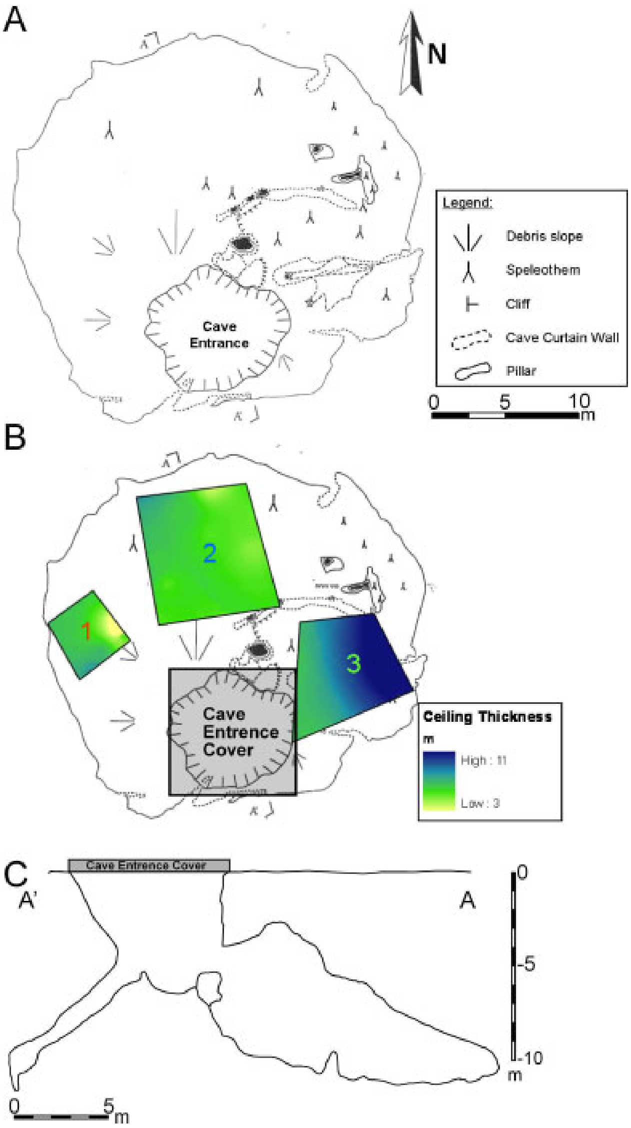

Figure 2. A. A map of Sif cave. B. The location of the three sheets collecting drip-water in the cave, and the cave ceiling thickness above each collection sheet. C. AA' section in Sif cave. The bright color in Site 1 indicates the karst chimney location

nature of the chamber cave allowed surveying the cave and ceiling using an EDM total station for high accuracy. The only known entrance into the cave is through a hole in the ceiling. This opening (9 m in diameter) was created during infrastructure development at the industrial zone during 1998 which truncated the top of a dome within the southern part of the cave. This entrance is now sealed with a door that is level with the surface of the ground and is opened only when entering the cave for equipment maintenance. The door was installed to prevent gross change in air circulation, maintain the natural high humidity levels, and thus minimize evaporation in the cave. At some locations in the cave, dissolution chimneys extend up from the ceiling, penetrating almost all the way up to the land surface.

Isolated chamber caves in the region are commonly decorated with speleothems which have been shown to be active throughout the Holocene and earlier periods (Frumkin *et al.*, 1999). This infiltration is a hydrological connection with the overlaying epikarst and, therefore, such caves are good locations for observing active aquifer recharge as it passes from the ground surface and down towards the phreatic zone (Frumkin *et al.*, 2009).

## METHODS

### *Natural rainfall events*

Daily rain was gauged at Barqan, 300 m NW of the cave, using a 0·2 mm resolution tipping bucket connected to a HOBO® data logger.

Drips were collected by three large plastic (polyvinyl chloride, PVC) sheets which integrate hundreds of active drips from three different areas in the cave (Figure 2). The PVC sheet surface areas were: Site 1: 17 $m^2$, Site 2: 56 $m^2$, and Site 3: 46 $m^2$. The sheets channelled water into three separate barrels (0·53 $m^2$ area, 0·80 m high) each equipped with a pressure transducer, recording water height with a 5-min temporal resolution (Figure 3). The sheets slope steeply toward the barrels to minimize flow time. Valves (0-pressure electric taps) were installed at the bottom of each barrel and controlled by a floating device: once a barrel filled up, the float would cause the tap to open, allowing water to drain out until the float reached a minimum elevation causing the tap to close. The continuous direct measurement gives the rate and volume of mean aerial dripping for each of the three areas. The PVC sheet at Site 1 (4·0 × 4·2 $m^2$) was placed under a ceiling with a 1 m diameter chimney extending to 3 m below the land surface. Site 2 (7·0 × 8·0 $m^2$) and Site 3 (5·4 × 8·5 $m^2$) were placed under a speleothem-covered ceiling. The roof thickness is approximately 6–7 m above Site 1 and Site 2, and 8–11 m above Site 3 (Figure 2).

### *Artificial irrigation and tracer experiments*

In addition to natural rainfall events, artificial irrigation was applied during the dry season (Figure 4). The irrigation system consisted of seven water sprinklers

Figure 3. The collection sheet at Site 2, funnelling the drip water into a barrel at the far end of the sheet. This barrel is equipped with a pressure transducer connected to a 5 min interval data-logger, recording the water level in the barrel. Note the ceiling, densely decorated by speleothems

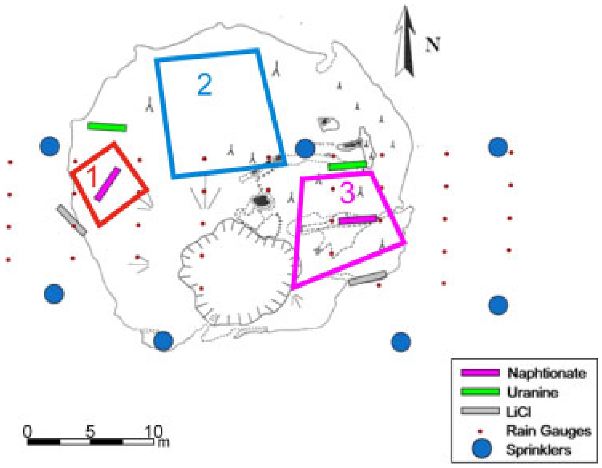

Figure 4. Layout of irrigation and tracer experiments above Sif cave. The tracers were injected into 20 cm wide hand dug trenches above and off the edge of the collecting sheets

Table I. Applied irrigation values (mm) and duration (hours) during the three experiments and the total drip collected during these experiments in mm and as a percent of applied irrigation. The total cave drip is the cumulative drip of all successive events

| Date | Irrigation (mm) | Duration (hr) | Total cave drip (mm) | % from cumulative irrigation (mm) |
|---|---|---|---|---|
| 16 Sep 2007 | 74·5 | 15 | 0 | 0 of 74.5 |
| 24 Sep 2007 | 41·8 | 3 | 2 | 2 of 116.3 |
| 30 Sep 2007 | 76·1 | 5 | 21 | 11 of 192.4 |

placed above the cave surface to produce intensities of 5–20 mm $h^{-1}$ (Table I). An array of 37 containers, used as accumulative rain gauges, were placed above the cave to monitor spatial distribution of irrigation.

A tracer experiment was conducted to track movement of water from the ground surface to the cave drips. Observation of the tracers in the cave could properly define the contributing surface area to the monitored sites in the cave and test the assumption of vertical flow in epikarst. The tracer experiment was conducted during the third irrigation experiment (30 Sep 2007) after soil water content was shown to have reached field capacity to saturation by the activation of the cave drips on the second irrigation. Prior to the third irrigation experiment, solutions of three tracers (Uranine, Na Naphtionate, and LiCl, detailed quantities are listed on Table II) were placed in shallow 20 cm deep hand dug ditches. The tracer Na Naphtionate was placed directly above Sites 1 and 3 as a control to determine whether the tracers actually percolate and were found at the sites; Uranine was placed 1 m north of the edge of the sheets; and LiCl was placed 1 m south of the edge of the sheets (Figure 4) to track north and south oblique movement of water. The two sites are located directly east–west, so that east and west movements were also monitored. The Uranine north of Site 1 was placed in an area believed to be the upper end of the preferred flow path leading to the dissolution chimney. Uranine and Na-Naphtionate have a low tendency to adsorb. Li however tends to adsorb (Sullivan *et al.*, 2003); therefore, large quantities were used to ensure partial recovery of Li as shown by Magal *et al.* (2007). Water samples were collected as water was flowing off the PVC sheets, before entering the barrels. Background values were taken just before the tracers were introduced (Table II).

Table II. Mass of tracers used and background values measured both at the domestic water source tap and in the cave prior to the experiments

| Tracer type | Amount injected (g) | Tap-water background concentration (ppb) | Drip-water background concentration (ppb) |
|---|---|---|---|
| Uranine | 10 | 0.0 ppb | 0.0 ppb |
| Na-Naphtionate | 100 | 0.0 ppb | 0.0 ppb |
| LiCl | 250 | 10.0 ppb | 0.3 ppb |

## RESULTS

### *Natural rainfall events*

Percolation at Site 1 is an order of magnitude higher than percolation at Sites 2 and 3 (Figure 5). When examining variations in hydrographs slopes on semi-log plots three flow regimes can be distinguished at Site 1, but only two flow regimes can be distinguished at Sites 2 and 3. The two flows are apparent in all three sites, and at Site 1 an additional flow regime exists (Figure 6). An increase in overall cave-drip activity throughout the rain season can be seen (Figure 5). The cave drips do not react to rain events at the beginning of the year, until a threshold of ~100 mm is reached. At the beginning of the rain season (September) 0% of the rainfall percolates into the cave. The first cave-drip response is after the ~100 mm threshold is passed (Figure 5). Further along into the rain season (December) only 5–10% of the rainfall percolates, slowly rising towards the end of the rain season (April), when 70–80% of rainfall percolates. An annual recharge of 140–160 mm (30–35% of precipitation) was recorded in different areas in the cave. Close examination of the drip hydrographs shows that the lag time between a rain event and cave response decreases throughout the year. The first cave response (December) occurs 28–34 h after rain commences, and this lag time decreases to merely 4 hr by the end of the rain season (April).

### *Irrigation experiment*

Three artificial rainfall experiments were conducted in September 2007 over a 500 $m^2$ area above the cave (Figure 4). The initial soil moisture conditions were arguably minimal (Table I, Figure 7) since the last recorded rain event 5 months previously was in March (Figure 5).

The three experiments (Figure 7) were separated by a week to mimic the natural rainfall regime and to avoid discharge events overlapping. The experiment equipment

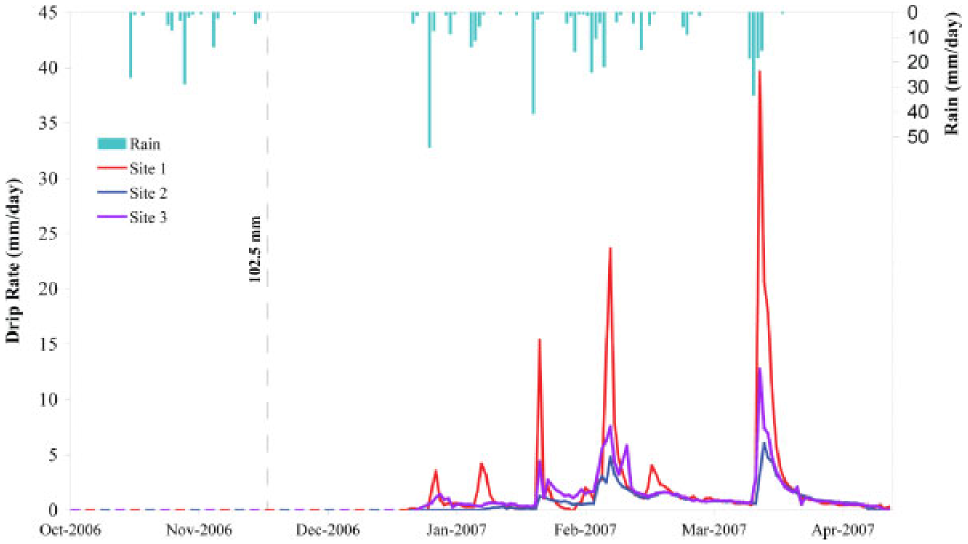

Figure 5. A drip hydrograph of the three sites at the cave, with associated rainfall during 2006–2007 (values were normalized in accordance with sheet size). Site 1 exhibits drip rates higher by an order of magnitude in relation to Sites 2 and 3. The high rate is due to 'Quick flow' through preferred flow path. All sites produce no drip before a 100 mm threshold is reached and then a general rise in drip rate of consecutive events throughout the rain season (monitoring of the cave drip shows no activity during, and as a result of, the rain in October and November)

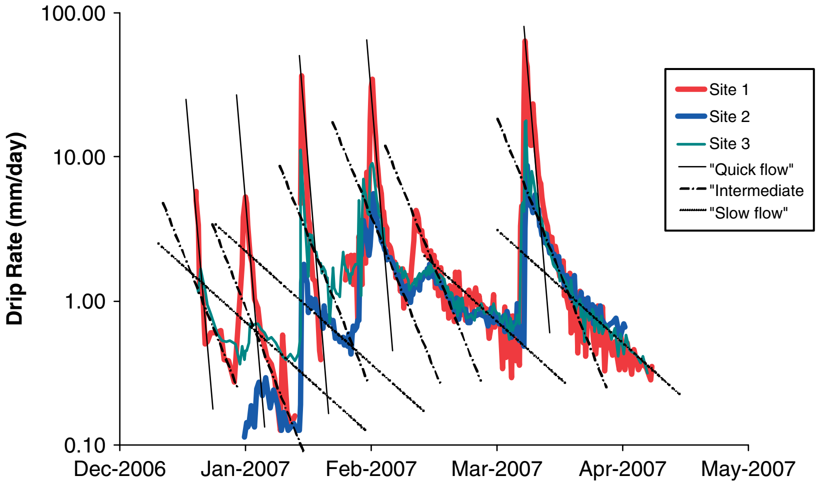

Figure 6. Drip hydrograph rates presented on a semi-log graph. This enables differentiation of three flow regimes: a 'Quick flow' (solid line), recorded only at Site 1; 'Intermediate flow' (dashed); and 'Slow flow' (dotted line). 'Intermediate' and 'Slow' flows were identified at all three sites

enabled irrigation only over Sites 1 and 3. As in the natural rainfall events, only after a cumulative 100 mm of irrigation was applied did the cave drips become active in response to the irrigation (Figure 8). Therefore, the first irrigation of 75 mm, resulted in no drips; the second event of 42 mm produced a total drip of 2 mm after achieving the threshold required by accumulating 116 mm; and the final event of 76 mm produced a large response in the cave (Figure 8; Table I).

### *Tracer experiment*

Tracers were introduced after the second irrigation once 116 mm of irrigation had been applied to overcome the recharge activation threshold. With the now wetted hydrologic connection to the cave the three tracers of Uranine, Na Naphtionate, and LiCl, were placed in the trenches above the cave at Sites 1 and 3 as described in section 3·2 (Figure 4).

The Na Naphtionate placed directly above the center of the sites was recovered after 23 and 29 h at Sites 1 and 3, respectively (Figure 9). Average ceiling thickness at Sites 1 and 3 are 7 and 9 m, respectively, indicating flow velocities of 0·32 m h$^{-1}$ at both sites.

The Uranine was released in trenches 1 m north of the edges of the PVC sheets on the ground surface. At Site 1, Uranine was recovered 5 h from the beginning of the irrigation experiment at high concentrations (Figure 9(a)). Ceiling thickness at the chimney is approximately 3 m, the Uranine was placed approximately 5 m horizontally from the chimney, resulting in a minimal distance of ~6 m indicating minimum flow rate of 1·2 m h$^{-1}$. Total Uranine recovery following the experiment was approximately 20% at Site 1. Although the mass of Na-Naphtionite used was 10 times greater than the Uranine used, the Uranine concentrations in the cave were 3 orders of magnitude higher than the Na-Naphtionite.

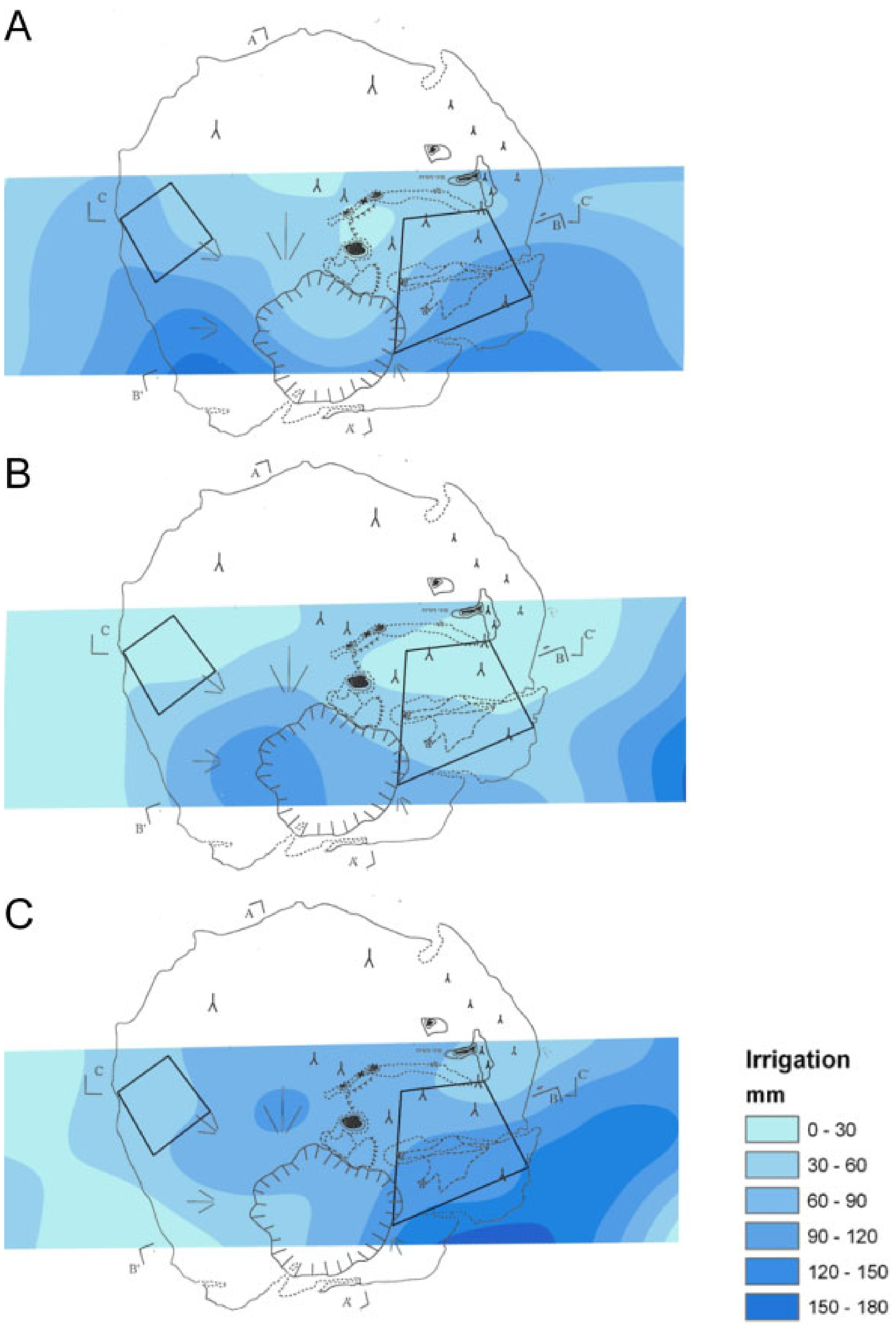

Figure 7. Maps of artificial irrigation showing the spatial distribution of the artificial rain during 2007 experiments: A. 16 Sep. for 15 h; B. 24 Sep. for 3 h; and C. 30 Sep. for 5 h

Samples collected months later into the next rain season contained some Uranine too. The Uranine was not recovered at Site 3. LiCl released in a trench 1 m south of the edge of the PVC sheets on the ground surface was not recovered at any of the sites, keeping low and stable background levels as measured prior to the experiment.

## DISCUSSION

The Sif Cave study presents a unique window to observe vadose zone percolation to the WMA. The ~100 mm threshold required to activate cave drip at the beginning of the rain season is the amount required to raise soil moisture content from near wilting point (after a long dry summer) to field capacity values. Having a soil cover thickness of 0·6–0·7 m, above the cave, receiving 100 mm of rain constitutes ~15% soil moisture which is the difference between wilting point (17%) to field capacity (32%) in terra rossa soil (Dingman, 1994). This value closely resembles previous studies such as Arbel *et al.* (2008), who calculated a threshold of 120 mm for Mt Carmel caves. Any amount above field capacity

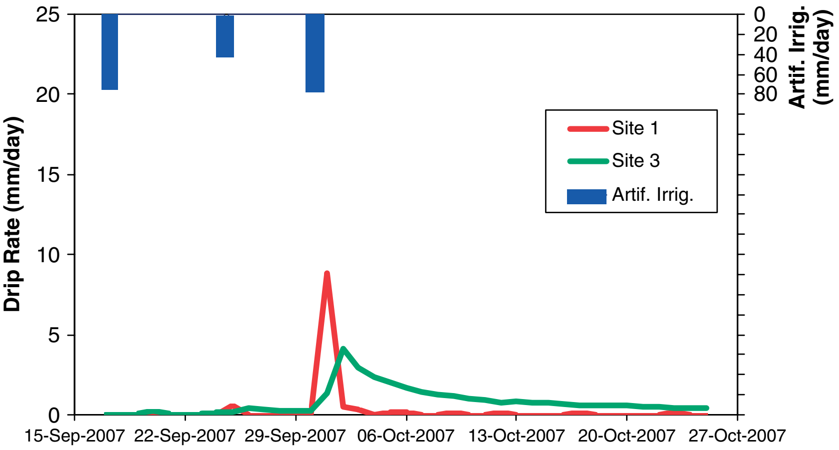

Figure 8. The drip hydrograph of the irrigation experiments. The first two artificial rain events had almost no effect on the dripping. Dripping started in the cave only after the ~100 mm threshold was reached by the artificial rain

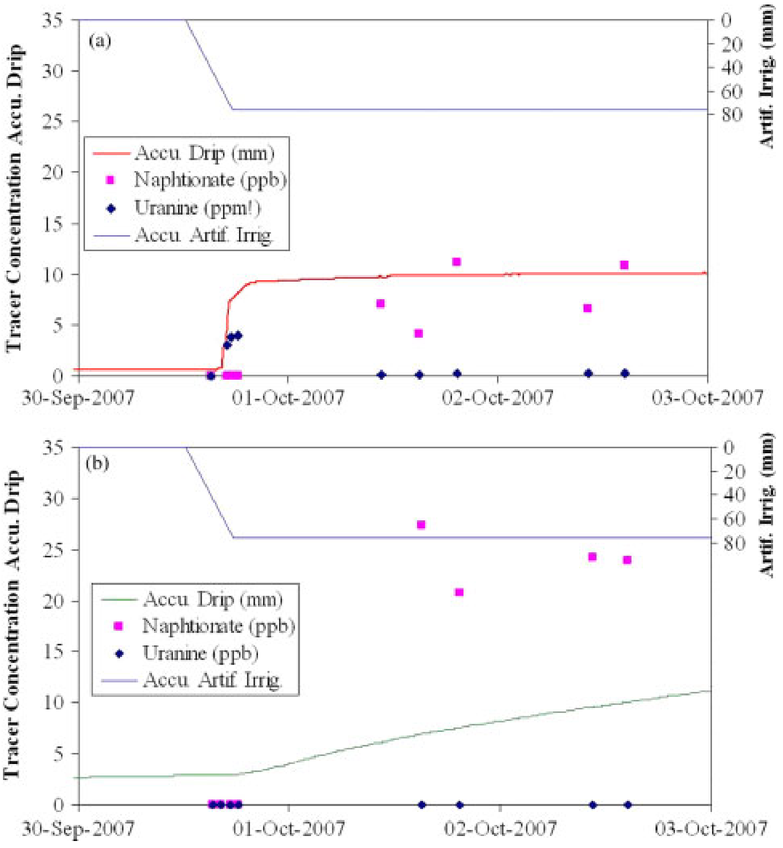

Figure 9. Dye concentrations observed in cave drip water after irrigation over shallow release ditches with dye release of dye. A) Site 1, B) Site 3. For Sites 1 and 3, the naphtionite dye was released in trenches directly above the collection sheets, and was recovered 23 and 29 h post release for Sites 1 and 3 respectively. The LiCl and Uranine were released in separate trenches situated 1–2 m outside the edges of the collection sheets. The LiCl was not recovered at either of the sites. Uranine was not recovered at Site 3. At Site 1, the Uranine was released in a trench above the vadose chimney identified in the cave, and was recovered within 5 h. Note, that the initial drip values were not 0 (for the accumulated drip) because the cave was activated a week prior to the tracer experiment after the second irrigation experiment. The left *Y* axis represents both tracer concentrations in drip water and accumulated drip measured in the cave. The units are shown in the legend—note that concentrations for Uranine in 9A is in ppm, whereas, all other concentrations are in ppb

causes water movement from the soil to the subsurface epikarst. The soil moisture is removed either by draining water from the soil to the epikarst (for any amount above field capacity) or by ET, which depletes water eventually to the wilting point. The ~100 mm threshold is a result of the long dry summer depleting the soil and vadose moisture to a minimum, requiring the initial threshold value for the renewal of cave drips. Only after reaching the threshold the cave drips respond to rain events intermittently.

As rain season progresses, soil water content rises. This results in (i) increase in recharge per rain event, from 0% before field capacity is reached, through ~5–10% once the 100 mm threshold is reached, to 70–80% by the end of the rain season; and (ii) the decrease in lag time between rain events and cave drip response from 29–34 h to 4 h. The overall average annual recharge of 30–35% is consistent with long-term mean annual recharge values of the WMA (Gvirtzman, 2002).

The three flow regimes identified in the hydrographs represent the Quick flow, Intermediate flow and Slow flow (Figure 6). Repetition of the slope angle in each of the flow regimes indicates that recharge is governed by vadose zone characteristics. Quick flow is recorded solely at Site 1 and is attributed to flow through large conduits in the rock and the karst chimney (aven) above this site. The Intermediate and Slow flows were recorded at all three sites, indicating that the rock covering the cave has an evenly spatially distributed fissure network, and matrix. The additional Quick flow recorded at site 1 indicates the presence of a much larger local developed fracture system.

Tracer experiments enabled (1) calculation of subsurface flow rates; and (2) testing the assumption of vertical flow required for recharge calculations.

The similarity in results at sites 1 and 3 (flow rate of 320 mm $h^{-1}$) indicates that the karst medium in the vicinity of the cave is an evenly spatially distributed dual crack and fissure network. This flow constitutes the Slow flow regime. The short travel time and high concentration measured at Site 1 points to the Quick flow regime through preferred flow paths. Rates of water movement range from 320 mm $hr^{-1}$ for the Intermediate/Slow flow to $>$1200 mm $hr^{-1}$ for Quick flow. Although a large range of rates exist in karst environment studies, the slow flow value resembles recent karst recharge studies conducted in Israel resulting with 220–400 mm $h^{-1}$ at Mt Carmel caves (Arbel Y, *et al.*, 2008).

The tracer experiment was set up with different tracers placed north (Uranine) and south (LiCl) of the cave drip water collection sites. The use of different tracers was to identify southbound and northbound movement by identifying recovery of the two tracers. The absence of Uranine and LiCl recovery (apart from the preferred flow path of Uranine at Site 1), strengthens our confidence in the assumption of no northbound or southbound flow components. The Uranine recovered in Site 1 was a result of Quick flow movement. A lateral movement southbound of Intermediate or Slow flows would result in a second peak for Uranine at Site 1. The absence of a second peak (Figure 9(a)) supports the assumptions of no southbound movement. Li values measured in the sampled cave drip water, prior to the introduction of LiCl to the system, correlate to background values measured in the tap water. Absorbance of LiCl in the soil or rock would result in no Li in the cave. The unchanged Li values after introducing extremely high LiCl concentrations in the surface trench supports the assumption of no northbound component. (LiCl concentrations used were three orders of magnitude higher than tap-water values, which were detectable in the cave following the first irrigation experiment).

Furthermore, the lack of all three tracers reappearing at a later time at the cave allows the assumption of no westbound or eastbound flow components either. Therefore, vertical flow can be assumed at the study site allowing water budget calculations to be conducted.

Although the cave is limited in area it produces similar results to those known for the WMA. This study is unique in its approach to integrate a drip area of approximately 120 $m^2$ in a cave. This spatial integration produces a representative understanding of recharge processes through the epikarst for this area. Previous studies that concentrated on either single speleothems or a limited group of speleothems with the aim of understanding for capture of paleoclimate records in speleothems may have missed aspects of the flow regimes present at the study site, whereas in this study, integration of recharge waters allowed distinction of three different flow regimes at a local site of value in efforts of water resource managements.

Studying the water percolation and understanding the fundamental processes that govern recharge lay the foundations for the WMA model—DReAM which uses assumptions and processes based on field studies (Sheffer *et al.*, 2010). These assumptions include the threshold for water percolation; the gradual rise in recharge as the rain season progresses and the effect of dry periods on soil water content. Although the main factor governing recharge is rain (explaining $\geq$70% of variability), variability in the duration and intensity of precipitation produce different recharge values for years with similar total rain amounts. This variability was explained by incorporation of temporal data such as length of dry periods between rain events (explaining $\geq$90% of variability). This factor extends dry spells allowing depletion of soil moisture by *ET*, resulting in years with similar annual precipitation but with different recharge. The longer the dry spells, the less recharge produced.

Sheffer (2009) addresses the scaling issue showing that the regional scale (2200 $km^2$) and local scale (0·7–4 $km^2$) have similar recharge characteristics. Both regional and local scales are within the recharge zone of the WMA which is the location of this study site also. Consistency between the field studies and the model simulations indicate that although scaling cannot be extended from 120 $m^2$ (Sif Cave) to 2200 $km^2$, similar characteristics do exist in all scales, and local site specific studies in this case allow a better understanding of the recharge process.

## CONCLUSIONS

By high-resolution integrative drip rate recording, irrigation experiments and tracer tracking, an understanding of the different flow regimes in a small scale (120 $m^2$) dry Mediterranean epikarst was achieved.

1. Three separate flows regimes were defined according to cave drip hydrographs—Quick flow, Intermediate

flow and Slow flow. The Quick flow follows preferred flow paths such as may be through conduits, whereas Intermediate flows in a fissure system, and Slow flow percolates through the matrix. The Slow flow was calculated to be 300 mm $\mathrm{hr}^{-1}$ based on recovery of the tracer Na Naphtionate.

2. A threshold of 100 mm was found to be essential for dripping to initiate at the cave after the long dry summer season.
3. The lag time between rain events and cave dripping decreases throughout the rain season from 29–34 h to 4 h.
4. Recharge rate increases for each rain event throughout the winter, beginning with no recharge until the 100 mm threshold is reached, and then increasing up to 70–80% of precipitation.
5. The spatial pattern of tracer recoveries support the general assumption of vertical flow through the vadose zone, allowing recharge calculations to be conducted. Annual recharge to the cave was 140–160 mm, representing 30–35% of annual precipitation, similar to the long term average recharge for the WMA.
6. The fundamental processes governing recharge to the cave are in agreement with processes described by models at local and regional scales.

## ACKNOWLEDGEMENTS

This project was funded by the Regional R&D center at Ariel and GLOWA—Jordan River Project funded by the German Ministry of Science and Education (BMBF), in collaboration with the Israeli Ministry of Science and Technology (MOST). The authors wish to thank the three anonymous reviewers for their insightful comments. The authors also wish to thank Bridget Scanlon for editing the manuscript, Tamar Soffer from the Cartography lab at the Geography department for map production, Shilo Navon, Erez Beit Halachmi, Shahar Rozalis, Hagit Tamari, Yoni Bahat, Yael Yaakobi, Annie Geller, Yona Geller and Elad Dafny for assistance in field work.

## REFERENCES

Arbel Y, Greenbaum N, Lange J, Shtober-Zisu N, Grodeck T, Wittenberg L, Inbar M. 2008. Hydrologic classification of cave drips in a Mediterranean climate, based on hydrograph separation and flow mechanisms. *Israel Journal of Earth Sciences* **57**(3–4): 291–310.

Arkin Y. 1967. Explanations to geological map of Jerusalem-Bet Shemesh area. *Israel Journal of Earth Sciences* **16**(1): 46.

Bakalowicz MJ, Jusserand C. 1987. Etude de l'infiltration en milieu karstique par les methodes geochemiques et isotopiques. Cas de la Grotte de Niaux. *Bulletin du Centre d'Hydrogeologie, Universite Neuchatel*, **7**: 265–283.

Baker A, Brunsdon C. 2003. Non-linearities in drip water hydrology: an example from Stump Cross Caverns, Yorkshire. *Journal of Hydrology* **277**(3–4): 151–163.

Bottrell SH, Atkinson TC. 1992. *Tracer study of flow and storage in the unsaturated zone of a karstic limestone aquifer*. Tracer Hydrology: Rotterdam, pp. 207–211.

Committee on Soil Classification Israel, 1979. The classification of Israeli soils, ARO, Bet Dagan, Israel.

Dahan O, Shani Y, Enzel Y, Yechieli Y, Yakirevich A. 2007. Direct measurements of floodwater infiltration into shallow alluvial aquifers. *Journal of Hydrology* **344**(3–4): 157–170.

Dingman SL. 1994. *Physical hydrology*. Prentice-Hall, Inc.: Upper Saddle River, New Jersey.

Eaton RR, Bixler NE. 1987. Analysis of a multiphase, porous-flow imbibition experiment in fractured volcanic tuff. In *Flow and Transport Through Unsaturated Fractured Rock*, Evans DD, Nicholson TJ (eds). Geophysical Monograph. Ser. AGU: Washington, **42**: 91–98.

Even H, Carmi I, Magaritz M, Gerson R. 1986. Timing the transport of water through the upper vadose zone in a karstic system above a cave in Israel. *Earth Surface Processes and Landforms* **11**: 181–191.

Fischhendler I, Frumkin A. 2008. Distribution, evolution and morphology of caves in south-western Samaria, Israel. *Israel Journal of Earth Sciences* **57**: 311–322.

Ford D, Williams P. 2007. *Karst hydrogeology and geomorphology*. Wiley: West Sussex, England, pp. 562.

Friederich H, Smart PL. 1982. The classification of autogenic percolation waters in karst aquifers: A study in G.B. cave, Mendip Hills, England. *Proceedings of the University of Bristol Speleological Society* **16**(2): 143–159.

Frumkin A. 1984. *Karst shafts in a Mediterranean environment*, The Hebrew University of Jerusalem: Jerusalem.

Frumkin A, Carmi I, Gopher A, Ford DC, Schwarcz HP, Tsuk T. 1999. A Holocene millennial-scale climatic cycle from a speleothem in Nahal Qanah Cave, Israel. *Holocene* **9**(6): 677–682.

Frumkin A, Fischhendler I. 2005. Morphometry and distribution of isolated caves as a guide for phreatic and confined paleohydrological conditions. *Geomorphology* **67**(3–4): 457–471.

Frumkin, A, Karkanas P, Bar-Matthews M, Barkai R, Gopher A, Shahack-Gross R, Vaks A. 2009. Gravitational deformations and fillings of aging caves: The example of Qesem karst system, Israel. *Geomorphology* **106**(1): 154–164.

Goldreich Y. 1998. *The climate of Israel: observations, research and applications*. Bar Ilan University; Magnes Pub. The Hebrew University: Tel Aviv, p. 292.

Gregory L, Wilcox BP, Shade B, Munster C, Owens K, Veni G. 2009. Large-scale rainfall simulation over shallow caves on karst shrublands. *Ecohydrology* **2**(1): 72–80.

Gvirtzman H. 2002. *Israel water resources*. Yad Ben-Zvi Press: Jerusalem.

Hogan JF, Phillips FM, Scanlon BR. 2004. *Groundwater recharge in a desert environment: The southwestern United States*. *Water Science and Application* 9. AGU: Washington, p. 294.

Kogovšek J. 1997. *Water tracer tests in the vadose zone*. Tracer Hydrology: Balkema, Rotterdam.

Koons RD, Helmke PA. 1978. Neutron activation analysis of standard soils. *Soil Science Society of America Journal* **42**(2): 237–240.

Magal E, Arbel Y, Caspi S, Katz Y, Glazman H, Yechieli Y, Greenbaum N. 2007. *Tracer test in Ein Ziv, GSI/10/2007*, ISR. GEOL. SURV.: Jerusalem.

NRC. 2004. *Groundwater fluxes across interfaces*, National Research Council: Washington DC.

Quinlan JF, Davies GJ, Jones SW, Huntoon PW. 1996. The applicability of numerical models to adequately characterize ground-water flow in karstic and other triple-porosity aquifers. *Subsurface Fluid-Flow (Ground-Water and Vadose Zone) Modeling* **1288**: 114–133.

Rimon Y, Dahan O, Nativ R, Geyer S. 2007. Water percolation through the deep vadose zone and groundwater recharge: preliminary results based on a new vadose zone monitoring system. *Water Resources Research* **43**(5).

Sheffer NA. 2009. Variable scale recharge measurement and modelling using the hydrometeorological DReAM. PhD Thesis, The Hebrew University of Jerusalem, Jerusalem, Israel, p. 97.

Sheffer NA, Dafny E, Gvirtzman H, Frumkin A, Navon S, Morin E. 2010. The hydrometeorological DReAM (Daily Recharge Assessment Model) for the Israeli western mountain aquifer (WMA). *Water Resources Research* **46**: W05510, 16 pp. DOI:10.1029/2008WR 007607.

Sophocleous MA. 1991. Combining the soilwater balance and water-level fluctuation methods to estimate natural groundwater recharge—practical aspects. *Journal of Hydrology* **124**(3): 229–241.

Sullivan EJ, Reimus PW, Chipera SJ, Counce D. 2003. Effects of mineralogy, exchange capacity, surface area and grain size on lithium sorption to zeolitic alluvium near Yucca Mountain, Nevada. *Clays and Clay Minerals* **51**(6): 634–643.

Worthington SRH, Ford DC. 1999. Chemical hydrogeology of the carbonate bedrock at Smithville. Report to Smithville Phase IV Bedrock Remediation Program., Ontario Ministry of the Environment, Hamilton, Ontario.